IEEE Access
Multidisciplinary ⋮ Rapid Review ⋮ Open Access Journal

Received 14 March 2023, accepted 23 May 2023, date of publication 31 May 2023, date of current version 8 June 2023.

Digital Object Identifier 10.1109/ACCESS.2023.3281755

RESEARCH ARTICLE

A Novel Constellation Modification Method for Harmonic Modulated MPSK Data Transmission in Millimeter Wave Communication

ÖZGÜN ERSOY[1], MURAT CAN KARAKOÇ[1,2], AND ASAF BEHZAT ŞAHİN[1]
[1]Department of Electrical and Electronics Engineering, Ankara Yıldırım Beyazıt University (AYBU), Etlik, 06010 Ankara, Turkey
[2]Department of Electrical and Electronics Engineering, Erzurum Technical University, Yakutiye, 25050 Erzurum, Turkey

Corresponding author: Özgün Ersoy (ozgun.ersoy@ybu.edu.tr)

This work was supported in part by the Ankara Yıldırım Beyazıt University Scientific Research Projects Coordination Unit under Grant FDK-2022-2387, and in part by the Scientific and Technological Research Council of Turkey (TUBITAK) under Grant 122E409.

ABSTRACT The size of the data transmitted in communication systems is constantly increasing and leads to the need for high bandwidth. Therefore, using the millimeter wave (mmWave) band is one of the best solutions in data transmission. Frequency multiplication via nonlinear components is used for signal generation at higher frequencies in the millimeter to submillimeter bands and it is of great importance in generating signals up to 2.2 THz. Although communication systems with the highest carrier frequency using these components are available at the 300 GHz-340 GHz, standard communication models do not comply with data transmission at this band, bringing problems caused by nonlinearity throughout data recovery. We solve these problems with the proposed constellation modification method, which has not been studied before. In this study, it is aimed to provide data transmission in the mmWave band with an experimental communication system that is compatible with the frequency multiplication and has high spectral efficiency. For the first time to our knowledge, a novel constellation modification method that can be modified according to the frequency multiplication on the standard M-ary phase shift keying (MPSK) data is proposed. In this method, the existing receiver structure is preserved and MPSK with harmonic modulation is carried. In the experimental demonstration part, harmonic binary shift keying (BPSK) data transmission via frequency multiplied 30 GHz transmitter was achieved with a power penalty of 2.3 dB, and this shows that MPSK data transmission over harmonic mmWave or submillimeter band sources is now possible.

INDEX TERMS Constellation modification, harmonic modulation, mmWave communication, MPSK.

I. INTRODUCTION

Millimeter Wave (mmWave) spectrum allows for high data rates compared to lower frequency bands and is therefore considered for Fifth Generation (5G) wireless networks and beyond Fifth Generation (B5G). Moreover, it is anticipated that mmWave frequencies will have a key role in Sixth Generation (6G) wireless systems due to the huge available bandwidth of many tens of GHz [1]. As there is a great demand for more efficient and reliable usage of spectrum in 5G networks, many broadcast systems adopt the mmWave spectrum to make up for the shortage of spectrum resources [2], [3]. Thus, the huge available bandwidth offered by the mmWave band can provide the rates of multiple gigabit per second per user [2]. Despite the significant downsides of mmWave signals, such as limited coverage, signal blockages by obstacles, and severe signal attenuation caused by short wavelengths, it appears that the frequency band utilized to deliver high data rate traffic will inevitably be shifted to mmWave or even sub-terahertz (sub-THz) frequency bands [4], [5], [6]. Consequently, studies have been conducted on the mmWave band [7]. In our earlier research in which we investigated the effects of frequency upconversion through harmonic frequency multiplication on the transmitted digital data pulse shape and data rate in the mmWave band, we demonstrated that through pulse

The associate editor coordinating the review of this manuscript and approving it for publication was Olutayo O. Oyerinde.

shaping the transmitted data eye diagram signal to noise ratio (SNR) can be improved by 3 dB or data rate can be increased by 20% [8]. We conducted a separate research on the implementation of the faster than Nyquist (FTN) transmission method together with harmonic receiver, which aims to achieve high data rates with spectral efficiency in the terahertz communication band. As a result of the comparison of normal modulation with harmonic modulation, it is shown that the use of harmonic receiver enhances the system performance [9].

When the studies are examined in the literature, it can be observed that channel measurement, signal quality, transmission rate, and transmission coverage measurements are made at different frequencies in the mmWave spectrum. For example, a three-dimensional (3D) spatial statistical channel model for the mmWave and sub-THz frequencies was created based on measurements made in the line-of-sight (LOS) and non-line-of-sight (NLOS) scenarios in an indoor office building at 28 GHz and 140 GHz [1]. Moreover, penetration loss measurements were made for different materials at 28 GHz, 39 GHz, 120 GHz and 144 GHz, respectively [10]. Additionally, for the 5G systems, a channel sounding campaign at 70 GHz in an outdoor scenario is presented for broadband analysis of the multipath propagation channel in time-varying environments in the mmWave band [11]. In the indoor environment, Vector Network Analyzer (VNA) based channel sounding at 306 GHz and 321 GHz frequency was studied [12]. In this direction, channel sounding methods used in mmWave and THz bands are explained in [13]. After the studies in which channel properties were measured and analyzed in varying conditions, the signal quality and transmission coverage area of the 40 GHz mmWave band were examined in the indoor environment [3]. It can be seen from existing studies that direct signal generation near the THz band is not possible as there are no amplifiers and active balanced mixers in this frequency range [12], [14]. For this reason, signal generation in the THz band can only be achieved using frequency multiplier or frequency multiplier chain. In this way, obtaining a signal in the THz band by generating the harmonics of the input signal is accomplished with nonlinear devices such as Schottky diodes [15]. As an example, the carrier frequency was produced at 81 GHz with the x12 frequency multiplier chain starting from the 6.75 GHz carrier frequency in [11] and x12 frequency multiplier chain was employed in order to generate 140 GHz carrier frequency [1]. To obtain 301 GHz and 321 GHz carrier frequencies in an indoor channel sounding setup, x24 and x27 frequency multiplier chains were utilized [12]. E-band mmWave propagation is studied on the link over sea, where the distance between transmitter and receiver is 12 km and 74 GHz carrier frequency was achieved using the x6 multiplier chain [16]. In another study in the E-band, the carrier frequency was upconverted to 78 GHz using the x8 multiplier chain [17]. Although frequency multiplier chains are utilized to generate signal for the mmWave and beyond in many studies, 60 GHz transmitter and receiver structures are available in the market [18], [19], [20], [21].

The signal generation in the mmWave band is provided by using frequency multiplier chains, however, various problems arise in data transmission due to nonlinear effects when standard communication models are used. For this reason, instead of providing data transmission at the desired operating frequency with an upconversion process using the local oscillator (LO) multiplier chain, which is applied in the studies in the literature, we applied harmonic modulation, which provides data transmission at the desired operating frequency by generating the harmonics of the modulated signal. Commercially available high frequency (>100 GHz) transmitters are usually based on frequency multipliers in which only On-Off modulation is employed since it is not affected by the nonlinear nature of harmonic operation. In this study it is shown that BPSK or MPSK modulation of harmonic multiplier based transmitters is possible thanks to the proposed constellation modification method. Since harmonic modulation is applied, a novel constellation modification method that can be modified according to the frequency multiplication technique on the standard MPSK data is used and providing data transmission in the mmWave band with an experimental communication system that is suitable for the frequency multiplication technique is aimed. The Universal Serial Radio Peripheral (USRP) is used while conducting our study experimentally for this purpose. USRP is a type of software defined radio (SDR) used in many areas from FM radio to mmWave 5G and beyond applications [22], [23], [24]. All signal processing methods in a wireless communication system are carried out with software which runs on a hardware on the SDR easily. A wireless communication system in a specified frequency range and channel bandwidth provided by the hardware is designed on the software and is implemented on the hardware in the SDR without difficulty. Accordingly, the 26-28 GHz mmWave platform presented for trial in SDR and the motivation of this setup have enabled the mmWave trial with a relatively simple system setup [25]. In addition to this, mmWave testbed was constructed using 60 GHz Tx/Rx RF front ends [18], USRP N210 and USRP N310 models [26], [27]. Also, the channel sounding was performed simultaneously at 3.2 GHz, 34.3 GHz, and 62.35 GHz using USRP to obtain the time-variant channel transfer function, and the carrier signals were obtained using x2 and x4 frequency multipliers from the 14.5 GHz LO signal, respectively [28]. In line with these studies, using the proposed novel constellation modification method, MPSK data transmission with harmonic modulation at 30 GHz has been experimentally realized.

The rest of the paper is organized as follows. In Section II, the proposed methodology for the modified MPSK data transmission in accordance with harmonic modulation in the mmWave band is discussed and analysis of the average BER performance for harmonic modulated MPSK in the presence

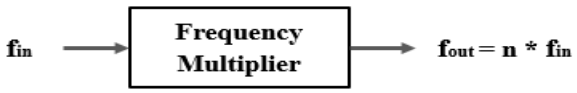

FIGURE 1. Block diagram of frequency multiplier.

of phase noise is performed. In Section III, the system model of experimental setups using USRP, and the real time mmWave testbeds are described, and in Section IV, the test outputs are discussed. Finally, in Section V conclusions inferred and future studies are given.

II. PROPOSED METHODOLOGY

A. HARMONIC MODULATION

In the mmWave communication systems, modulation, pulse shaping, and filtering are first done in lower frequency bands, then carried to higher frequency bands. In the frequency multiplication method, a system with nonlinear response produces the harmonics of the input signal and after filtering the desired multiplier coefficient is obtained. To achieve this goal, whereas active frequency multipliers such as nonlinear transistors and amplifiers are utilized in the RF band, Schottky diode based passive frequency multiplier structures are used for the mmWave and beyond because of their efficiency. Schottky Diode based components are employed either to upconvert these active components to THz band or to downconvert THz signals to lower frequencies. The nonlinear characteristics of Schottky diodes allow for conversion of the incident signal and multiplying its frequency. The nonlinearity of Schottky diodes can be used for generating harmonics of the incident signal. Thus, exact multiple harmonics of the incident signal can be obtained at the output of the nonlinear circuit. The harmonic modulation broadens the spectrum and power spreads to higher frequencies. Fig. 1 shows a block diagram of the frequency multiplier. The frequency multiplication is realized using nonlinear current-voltage (I-V) and capacitance-voltage (C-V) characteristics. The charge-voltage (Q-V) characteristic of Schottky diode can be defined in terms of power series [29].

$$Q\left(V\left(t\right)\right) = A_0 + A_1 V\left(t\right) + A_2 V(t)^2 + A_3 V(t)^3 + \ldots \quad (1)$$

Taking the derivative of (1), current equation can be derived.

$$I\left(t\right) = \frac{dQ(t)}{dt} = [A_1 + 2A_2 V\left(t\right) + 3A_3 V(t)^2 + \ldots]\frac{dV(t)}{dt} \quad (2)$$

In (1) and (2) A_0, A_1, A_2, and A_3 represent the coefficients of power series expansion. When the incident signal is a sinusoidal one, it can be observed that current and voltage equations are formed of its harmonics. The harmonic modulation in communication systems is called as generation of the harmonics of the modulated signal derived from (1) and (2).

If the modulated signal is mathematically expressed by $s\left(t\right) = m\left(t\right).A_c.cos\left(2\pi f_c t + \theta_c\right)$, then the harmonic modulated signal is written by

$$\begin{aligned} S_{Har.Mod}\left(t\right) &= m\left(t\right).A_c.cos\left(2\pi f_c t + \theta_c\right) \\ &\quad + [m\left(t\right).A_c.cos\left(2\pi f_c t + \theta_c\right)]^2 \\ &\quad + [m\left(t\right).A_c.cos\left(2\pi f_c t + \theta_c\right)]^3 \\ &= m\left(t\right).A_c.cos\left(2\pi f_c t + \theta_c\right) \\ &\quad + \frac{A_c^2.m^2\left(t\right)}{2}\left(1 + cos\left(2.2\pi f_c t + 2\theta_c\right)\right) \\ &\quad + \frac{A_c^3.m^3\left(t\right)}{4}\left(3.cos\left(2\pi f_c t + \theta_c\right)\right) \\ &\quad + \frac{A_c^3.m^3(t)}{4}\left(cos(3.2\pi f_c t + 3\theta_c)\right) \end{aligned} \quad (3)$$

which can be simplified as

$$\begin{aligned} S_{Har.Mod}\left(t\right) &= \frac{A_c^2.m^2\left(t\right)}{2} \\ &\quad + \left(m\left(t\right).A_c + \frac{3A_c^3.m^3(t)}{4}\right)cos(2\pi f_c t + \theta_c) \\ &\quad + \frac{A_c^2.m^2\left(t\right)}{2}cos\left(2.2\pi f_c t + 2\theta_c\right) \\ &\quad + \frac{A_c^3.m^3(t)}{4}cos(3.2\pi f_c t + 3\theta_c) \end{aligned} \quad (4)$$

In (4), $m(t)$ is the message signal, A_c is the amplitude of the modulated signal. The first term on the right side is the amount of dc voltage multiplied by square of $m(t)$ resulting from nonlinearity of second order, the second term is called the fundamental, the third term is called the second harmonic, and the fourth term is called the third harmonic. In the harmonic modulation, a system with nonlinear response produces the harmonics of the modulated input signal and after filtering the desired harmonic coefficient is obtained. If the harmonic modulation having a square characteristic is used, modulation at twice the carrier frequency is obtained. Low frequency source signal can be upconverted to high frequency band using frequency multiplication method. The frequency multiplier circuits are expected to generate enough power for a couple hundred GHz bandwidth as Schottky diode technology develops more.

B. A NOVEL CONSTELLATION MODIFICATION METHOD FOR MPSK

In the standard MPSK modulation, M carriers with equally distributed phases are used. The MPSK modulated signal is defined by [30]

$$S_{MPSK}\left(t\right) = A_c.cos(2\pi f_c t + \frac{(2i-1).\pi}{M}),\ i = 1, 2, \ldots, M \quad (5)$$

where A_c is the modulated signal amplitude and M denotes the modulation order. The MPSK modulated signal is written

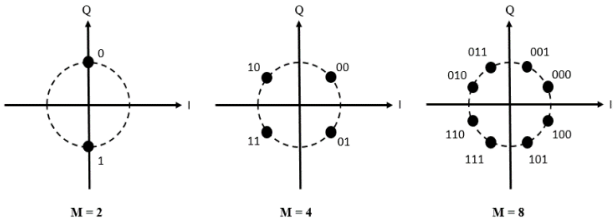

(a) BPSK (b) QPSK (c) 8PSK

FIGURE 2. Constellation diagrams for various MPSK modulations.

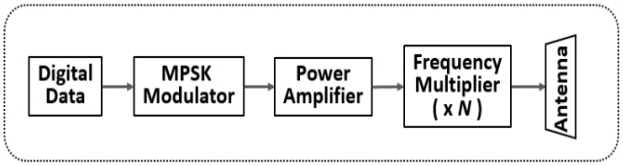

FIGURE 3. The block diagram of the frequency multiplication applied on MPSK signal.

by using trigonometric formulae in the interval of $0 \leq t \leq T_s$.

$$S_{MPSK}(t) = A_c.(cos(2\pi f_c t).cos\left[\frac{(2i-1).\pi}{M}\right] - sin(2\pi f_c t).sin\left[\frac{(2i-1).\pi}{M}\right]), \quad i = 1, 2, \ldots, M \tag{6}$$

This can be expressed as a combination of inphase and quadrature phase components on an I-Q plane. Inphase and quadrature phase components are used for a constellation diagram that shows the amplitude and phase values of carrier signals [31]. Normalizing the amplitude, the points on the constellation diagram are placed on the unit circle. The ideal constellation diagrams for $M = 2, 4,$ and 8 are shown in Fig. 2.

For the phase modulation types, the phase of the carrier signal is modulated. The effect of nonlinearities resulting from the frequency multiplication causes change in the phase information of the modulated data, also it leads to several problems which make it difficult to recover data at the receiver side for different types of phase modulation. The block diagram of the system accomplished for the frequency multiplication applied on the MPSK modulation is shown in Fig. 3.

When the frequency multiplication is applied, it becomes very hard to solve the data recovery problem with the existing receiver structure. This is due to the occurrence of a distortion in the phase modulation. Therefore, we propose the novel constellation modification for frequency multiplication used in the mmWave band communication systems to obtain high frequency signals. The distorted MPSK signal has the following mathematical expression at the output of the frequency multiplier block.

$$S_{Distorted\ MPSK}(t) = k.A_c^N.cos\left(2\pi N f_c t + \frac{(2i-1).\pi.N}{M}\right), \quad i = 1, 2, \ldots, M \tag{7}$$

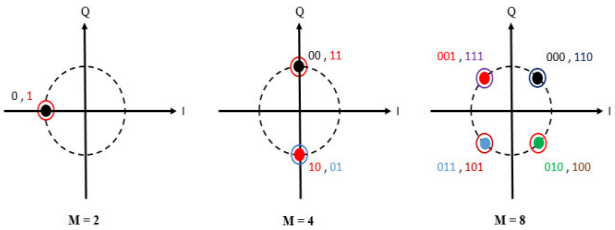

(a) Distorted BPSK (b) Distorted QPSK (c) Distorted 8PSK

FIGURE 4. Constellation diagrams of MPSK after frequency multiplication for $N = 2$.

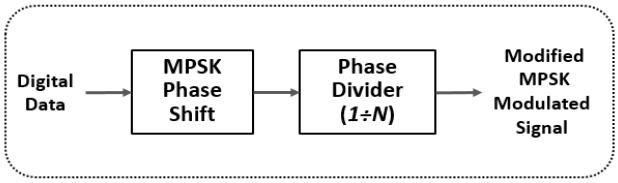

FIGURE 5. The proposed constellation modification for MPSK.

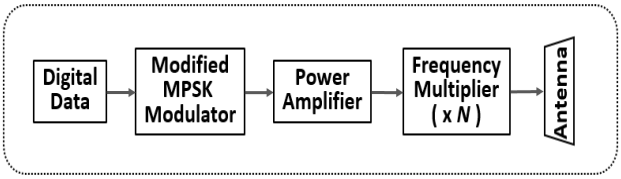

FIGURE 6. The block diagram of the frequency multiplication applied on the modified MPSK signal.

In the general form, the modulation order for MPSK is represented by M and the frequency multiplication factor by N. After the frequency multiplication, the distortion caused by the nonlinear effect can be observed in the constellation diagrams. When frequency doubler ($N = 2$) is used, the constellation diagrams for BPSK, QPSK and 8PSK are shown as an example in Fig. 4.

The novel constellation modification method is proposed to overcome the data recovery and phase distortion problems caused by harmonic modulation. Using this method, the constellation diagram of MPSK signals is modified, and the use of the modified MPSK signals ensures that the data are retrieved without any change in the receiver structure. The proposed Constellation Modification method is shown in Fig. 5.

The MPSK modulated signal has the following mathematical expression when the constellation modification is applied.

$$S_{Modified\ MPSK}(t) = A_c.cos\left(2\pi f_c t + \frac{(2i-1).\pi}{M.N}\right), \quad i = 1, 2, \ldots, M \tag{8}$$

The block diagram of the frequency multiplication applied on the modified MPSK signal is shown in Fig. 6.

When the frequency multiplier for $N=2$ is used, at the output of the constellation modification block, the constellation

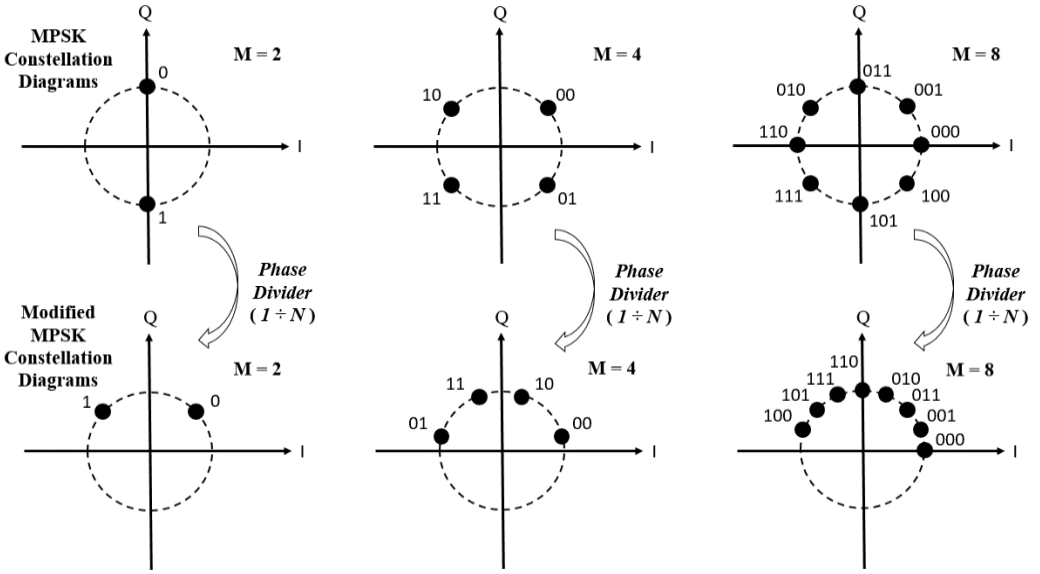

(a) Modified BPSK (b) Modified QPSK (c) Modified 8PSK

FIGURE 7. The constellation diagrams of modified MPSK before frequency multiplication.

diagrams of the modified MPSK for $M = 2, 4,$ and 8 are given as an example in Fig. 7. Depending on the modulation order, the phase shift of the carrier signal is divided by M for each symbol.

For example, in BPSK, the 90° phase shift is modified to 45° for the '0' symbol, while the 270° phase shift is modified to 135° for the '1' symbol. At the output of the Frequency Multiplication block, the modified MPSK signal has the following mathematical expression.

$$S_{Mod.MPSK.freq.mult.}(t) = k.A_c^N.cos\left(2\pi N f_c t + \frac{(2i-1).\pi.N}{M.N}\right) = k.A_c^N.cos\left(2\pi N f_c t + \frac{(2i-1).\pi}{M}\right), \quad i = 1, 2, \ldots, M \tag{9}$$

As an example, the constellation diagrams of the modified MPSK at the output of the frequency multiplier for $N=2$ are given for $M = 2, 4,$ and 8 in Fig. 8. When Fig. 8 is examined, it is seen that the constellation diagrams of the modified MPSK signals after frequency multiplication are transformed into the standard MPSK constellation diagrams. Thus, we do not need to change the receiver structure. The modified constellation is easy to generate and does not need higher bandwidth or digital processing load.

Before we evaluate the performance of our proposed constellation modification method, in the following section we first discuss the BER performance analysis of the MPSK with phase noise for the proposed method we considered in this paper.

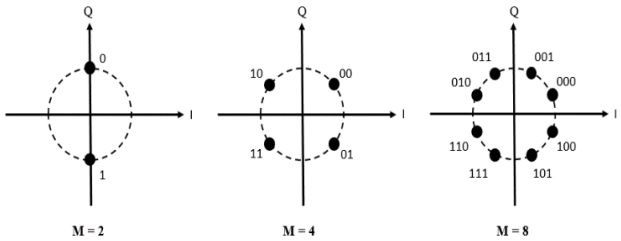

(a) Modified BPSK (b) Modified QPSK (c) Modified 8PSK

FIGURE 8. The constellation diagram of modified MPSK after frequency multiplication for $N = 2$.

C. BER ANALYSIS OF MPSK IN THE PRESENCE OF PHASE NOISE

Thanks to the offering large bandwidth of the THz band and the development of devices operating in this band, studies on mmWave communication systems are increasing. This brings along the use of multi-level modulation types such as MPSK to increase the data rate. In these systems where the carrier signals are produced using a local oscillator, one of the most significant factors affecting the BER performance of the system is the phase noise [32], [33]. The LO signal with phase noise is mathematically represented as:

$$S_{LO}(t) = A_{LO}.sin(2\pi f_{LO}(t) + \theta(t)) \tag{10}$$

where A_{LO} is the amplitude of LO signal, and $\theta(t)$ denotes the phase noise. Phase noise in communication systems can significantly affect their system performance, especially with high modulation orders. This is because the decision regions become smaller, and even slight phase deviations can cause errors in the signal. More specifically, the performance degradation increases as the modulation order increases.

Accordingly, MPSK is highly sensitive to phase noise, and BER performance analysis is crucial in evaluating its effectiveness [34], [35]. Especially, in regions with high SNR, the effect of phase noise on BER performance becomes dominant and results in an irreducible BER [32]. Moreover, when employing a frequency multiplier chain that multiplies the frequency by a factor of N, the phase noise becomes distorted by a factor of $20\ log_{10}N$ dB [36]. Additionally, using a mixer can also lead to phase noise [32]. Therefore, to ensure reliable and efficient transmission, it is important to consider the impact of phase noise and its effect on the BER performance of the system.

Numerous researches have provided either exact or approximate expressions for analyzing the BER performance of MPSK with phase noise because it is challenging to derive an average BER expression for MPSK [35], [37]. An approximate expression for the average BER of MPSK with Gaussian distributed phase error is derived in [35]. Additionally, an exact and general closed form expressions for the BER of MPSK in the presence of a fixed phase error are provided in [38]. Also, accurate expressions for the bit error probability (BEP) of Gray-coded M-ary rectangular and square QAM in the presence of phase noise in both AWGN and fading channels are presented in [39]. The effect of Gaussian phase noise on various waveforms is investigated and digital modulations in presence of phase noise are compared in [40]. Moreover, an approximate expression for the average BER of MPSK in a Nakagami-m fading channel, where a noisy phase reference exists is derived in [41]. Using the Tikhonov phase error model, the average symbol error rate performance of MPSK is analyzed [42]. Finally, to minimize the effect of oscillator phase noise on QPSK modulation in the AWGN channel, several estimators and corresponding results are proposed [43].

In an AWGN channel, the average BER of MPSK modulation in the presence of phase noise can expressed as [35]

$$P\left(e\right) = \int P\left(e \mid \theta\right).p\left(\theta\right).d\theta \tag{11}$$

where θ is phase noise, $P\left(e \mid \theta\right)$ is the conditional BER of MPSK with fixed phase noise, and $p(\theta)$ is the probability density function (PDF) of the phase noise. When assessing the error performance of coherent communication systems, it is common to assume that a perfect phase reference for demodulation is accessible to the receiver [44]. However, in practice, the local phase reference is reconstructed by utilizing a signal received with noise, which leads to a phase error typically modelled by Gaussian or Tikhonov [44] When there is phase noise present, the PDF of the phase noise can be modelled by a Tikhonov distribution, which is defined as

$$p\left(\theta\right) = \frac{e^{\alpha.cos\theta}}{2\pi I_0(\alpha)} \tag{12}$$

where α is the SNR in the loop bandwidth and also α^{-1} is the variance of θ and $I_n(.)$ is the n-th order modified Bessel function. In most cases, when the variance of θ is high, the PDF of the phase noise can be estimated using a Gaussian distribution, which is a straightforward and commonly used distribution and can be expressed as

$$p\left(\theta\right) = \frac{1}{\sqrt{2\pi\sigma^2}} e^{-\frac{\theta^2}{2\sigma^2}} \tag{13}$$

where σ^2 is the variance of θ. We assume that the phase noise has a Gaussian distribution, while performing BER performance analysis in this study. Accordingly, the MPSK signal with phase noise is defined as

$$S_{MPSK}\left(t\right) = A_c.cos\left(2\pi f_c t + \frac{\left(2i-1\right).\pi}{M} + \theta_{nt}\right), \quad i = 1, 2, \ldots, M \tag{14}$$

The received signal is represented by

$$\begin{aligned} r_t &= \left(S_{MPSK}\left(t\right).e^{j(2\pi ft+\theta_{nt})} + n_t\right).e^{j(-2\pi ft+\theta_{nr})} \\ &= S_{MPSK}\left(t\right).e^{j(\theta_{nt}+\theta_{nr})} + \hat{n}_t \end{aligned} \tag{15}$$

The terms θ_{nt} and θ_{nr} refer to the phase noise that is generated at the transmitter and receiver, respectively. $\hat{n}_t$ is the noise signal converted by the downconverter. Therefore, a rough mathematical expression for the conditional BER of MPSK, where the phase noise is distributed according to a Gaussian distribution and transmitted over AWGN channel, is derived as

$$P_{MPSK}\left(e \mid \theta\right) = \frac{2}{log_2 M}\sum_{i=1}^{\frac{M}{2}}\left(1 - erf\left(\sqrt{\frac{\varepsilon_b}{N_0}log_2 M}.\ sin\left(\frac{\left(2i-1\right).\pi}{M} + \theta_{nt} + \theta_{nr}\right)\right)\right) \tag{16}$$

Using trigonometric formulae, the expression in (16) can be expanded as

$$P_{MPSK}\left(e \mid \theta\right) = \frac{2}{log_2 M}\sum_{i=1}^{\frac{M}{2}}\left(1 - erf\left(\sqrt{\frac{\varepsilon_b}{N_0}log_2 M}.\left(sin\left(\frac{\left(2i-1\right).\pi}{M}\right).cos\left(\theta_{nt}+\theta_{nr}\right) + cos\left(\frac{\left(2i-1\right).\pi}{M}\right).sin\left(\theta_{nt}+\theta_{nr}\right)\right)\right)\right) \tag{17}$$

By substituting the mathematical equations given in (13) and (17) into (11), it is possible to compute the average BER expression for MPSK with phase noise distributed according to Gaussian distribution and transmitted over an AWGN

channel.

$$P_{MPSK}(e) = \int \frac{2}{log_2 M} \sum_{i=1}^{\frac{M}{2}} \left(1 - erf\left(\sqrt{\frac{\varepsilon_b}{N_0} log_2 M}.\left(sin\left(\frac{(2i-1).\pi}{M}\right).cos(\theta_{nt}+\theta_{nr}) + cos\left(\frac{(2i-1).\pi}{M}\right).sin(\theta_{nt}+\theta_{nr})\right)\right)\right). \frac{1}{\sqrt{2\pi\sigma^2}} e^{-\frac{\theta^2}{2\sigma^2}}.d\theta \quad (18)$$

Consequently, the presence of phase noise in the recovered carrier affects the MPSK signal, and the BER becomes dependent on both the SNR and the phase noise [45]. If we need to apply this process for the modified MPSK, the MPSK signal with phase noise is defined as

$$S_{Modified\ MPSK}(t) = A_c.cos\left(2\pi f_c t + \frac{(2i-1).\pi}{M.N} + \theta_{nt}\right), \quad i = 1, 2, \ldots, M \quad (19)$$

An approximate mathematical expression for the conditional BER of the modified MPSK with Gaussian distributed phase noise over an AWGN channel is derived.

$$P_{Modified\ MPSK}(e\,|\,\theta) = \frac{2}{log_2 M} \sum_{i=1}^{\frac{M}{2}} \left(1 - erf\left(\sqrt{\frac{\varepsilon_b}{N_0} log_2 M}.\ sin\left(\frac{(2i-1).\pi}{N.M} + \theta_{nt} + \theta_{nr}\right)\right)\right) \quad (20)$$

Using trigonometric formulae, (20) can be expanded as (21), as shown at the bottom of the next page.

Similarly, by substituting the mathematical equations given in (13) and (21) into (11), the average BER expression for the modified MPSK with Gaussian distributed phase noise over an AWGN channel is obtained as

$$P_{Modified\ MPSK}(e) = \int \frac{2}{log_2 M} \sum_{i=1}^{\frac{M}{2}} \left(1 - erf\left(\sqrt{\frac{\varepsilon_b}{N_0} log_2 M}.\left(sin\left(\frac{(2i-1).\pi}{N.M}\right).cos(\theta_{nt}+\theta_{nr}) + cos\left(\frac{(2i-1).\pi}{N.M}\right).sin(\theta_{nt}+\theta_{nr})\right)\right)\right). \frac{1}{\sqrt{2\pi\sigma^2}} e^{-\frac{\theta^2}{2\sigma^2}}.d\theta \quad (22)$$

The BER analysis for the modified MPSK was performed to clearly show the effect of the harmonic modulation on the modified MPSK. Our aim is to investigate the performance comparison between regular MPSK and harmonic MPSK. Ultimately, when we combine this procedure with the frequency multiplication method, we obtain the frequency multiplicated MPSK signal with phase noise, which can be expressed as

$$\begin{aligned} S_{Mod.MPSK.freq.mult.}(t) &= k.A_c^N.cos\left(2\pi N f_c t + \frac{(2i-1).\pi.N}{M.N} + \theta_{nt}.N\right) \\ &= k.A_c^N.cos\left(2\pi N f_c t + \frac{(2i-1).\pi}{M} + \theta_{nt}.N\right), \\ &\quad i = 1, 2, \ldots, M \end{aligned} \quad (23)$$

The received signal is represented by

$$r_{t,Mod.MPSK.freq.mult.} = S_{Mod.MPSK.freq.mult.}(t).e^{j.N.(\theta_{nt}+\theta_{nr})} + \hat{n}_t \quad (24)$$

A mathematical expression for the conditional BER of the harmonic modulated MPSK signal with Gaussian distributed phase noise over an AWGN channel is derived.

Using trigonometric formulae, (25), shown at the bottom of the next page, can be expanded as (26), shown at the bottom of the next page.

Likewise, by substituting the mathematical equations provided in (13) and (26) into (11), the formula for the average BER of the harmonic modulated MPSK with Gaussian distributed phase noise over an AWGN channel can be obtained as (27), shown at the bottom of the next page.

The analysis of the BER performance of MPSK with phase noise in the proposed method suggests that phase noise has a significant impact on the BER performance, resulting in a decrease in performance and a non-negligible power penalty. To demonstrate this, we conducted BPSK transmission simulations over an AWGN channel using MATLAB. The simulation generated BER curves for BPSK transmission with and without phase noise, which were compared. We also performed simulation to detect the effect of phase noise on the transmission of the harmonic modulated BPSK signal. For BPSK transmission, we used a frequency multiplication factor of $N=2$ during the simulation. The simulation results showed the BER performance for BPSK transmission with and without phase noise, as well as for harmonic modulated BPSK transmission. These results are presented in Fig. 9.

III. SYSTEM MODEL FOR EXPERIMENTAL SETUP IN mmWAVE BAND

In this study, the transmission of the regular and harmonic MPSK data in the mmWave band was performed. To achieve our objective, firstly, modulator structures separately for regular and harmonic MPSK data transmission were designed in the LabVIEW environment and performed in real time testbed using USRPs. Whereas the standard MPSK modulator is used for the regular MPSK data transmission, the modified MPSK modulator is used for the harmonic MPSK data transmission.

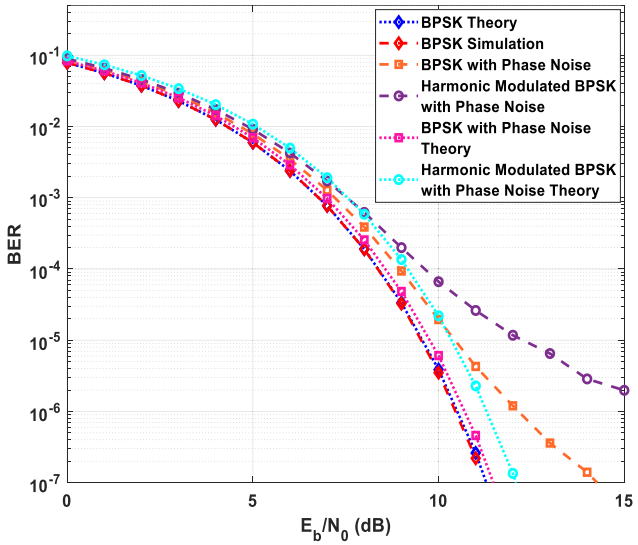

FIGURE 9. BER analysis of BPSK in AWGN channel with and without phase noise (frequency multiplication factor for harmonic modulation is $N = 2$.)

A. SDR IMPLEMENTATION OF THE STANDARD AND MODIFIED MPSK MODULATORS

The real-time performance analysis of the standard and the modified MPSK modulator was done by developing the transmitter and receiver blocks in the LabVIEW environment and tested using NI USRP-2922 models. The same USRP models were used as the receiver and transmitter, and the USRP MIMO expansion cable was used to provide clock and frequency synchronization between the USRPs. The MIMO extension outputs of the USRPs are connected to each other with a USRP MIMO expansion cable and the internal reference clock and frequency produced by one of the USRPs is shared with the other USRP. The standard MPSK transmitter and receiver structures implemented on the USRP for the regular MPSK data transmission is as in Fig. 10.

In Fig. 10(a), random bit generation is done at 50 kbps using the Fibonacci PN sequence order 11 in the LabVIEW. In addition, guard bits are used to prevent errors that may occur during successive measurements between the receiver and transmitter. These generated bits were modulated with MPSK and transmitted at a carrier frequency of 800 MHz. The gain parameter of the USRP can be adjusted so that the amplifier output power varies between -10 dBm and +20 dBm. Finally, after the MPSK demodulation given in Fig. 10(b), the BER analysis of the system operating at a carrier frequency of 800 MHz was made. The constellation diagrams obtained at the output of the standard MPSK modulator for BPSK and QPSK, which are shown in the LabVIEW environment, are given in Fig. 11. The USRP transmitter and receiver structures created using the constellation modification method for harmonic MPSK data transmission is shown in Fig. 12. Because the frequency multiplier with frequency multiplication factor of two doubles the phase information when the harmonic modulation

$$P_{ModifiedMPSK}(e\,|\,\theta) = \frac{2}{log_2 M}\sum_{i=1}^{\frac{M}{2}}\left(1 - erf\left(\sqrt{\frac{\varepsilon_b}{N_0}log_2 M}.\left(sin\left(\frac{(2i-1).\pi}{N.M}\right).cos\left(\theta_{nt}+\theta_{nr}\right) + cos\left(\frac{(2i-1).\pi}{N.M}\right)\right.\right.\right.$$
$$\left.\left.\left.\times\ sin\left(\theta_{nt}+\theta_{nr}\right)\right)\right)\right) \tag{21}$$

$$P_{Har.Mod.MPSK}(e\,|\,\theta) = \frac{2}{log_2 M}\sum_{i=1}^{\frac{M}{2}}\left(1 - erf\left(\sqrt{\frac{\varepsilon_b}{N_0}log_2 M}.sin\left(\frac{(2i-1).\pi}{M} + N.(\theta_{nt}+\theta_{nr})\right)\right)\right) \tag{25}$$

$$P_{Har.Mod.MPSK}(e\,|\,\theta) = \frac{2}{log_2 M}\sum_{i=1}^{\frac{M}{2}}\left(1 - erf\left(\sqrt{\frac{\varepsilon_b}{N_0}log_2 M}.\left(sin\left(\frac{(2i-1).\pi}{M}\right).\right.\right.\right.$$
$$\left.\left.\left.cos\left(N.(\theta_{nt}+\theta_{nr})\right) + cos\left(\frac{(2i-1).\pi}{M}\right).sin(N.(\theta_{nt}+\theta_{nr}))\right)\right)\right) \tag{26}$$

$$P_{Har.Mod.MPSK}(e) = \int \frac{2}{log_2 M}\sum_{i=1}^{\frac{M}{2}}\left(1 - erf\left(\sqrt{\frac{\varepsilon_b}{N_0}log_2 M}.\left(sin\left(\frac{(2i-1).\pi}{M}\right).cos\left(N.(\theta_{nt}+\theta_{nr})\right)\right.\right.\right.$$
$$\left.\left.\left.+cos\left(\frac{(2i-1).\pi}{M}\right).sin\left(N.(\theta_{nt}+\theta_{nr})\right)\right)\right)\right).\frac{1}{\sqrt{2\pi\sigma^2}}e^{-\frac{\theta^2}{2\sigma^2}}.d\theta \tag{27}$$

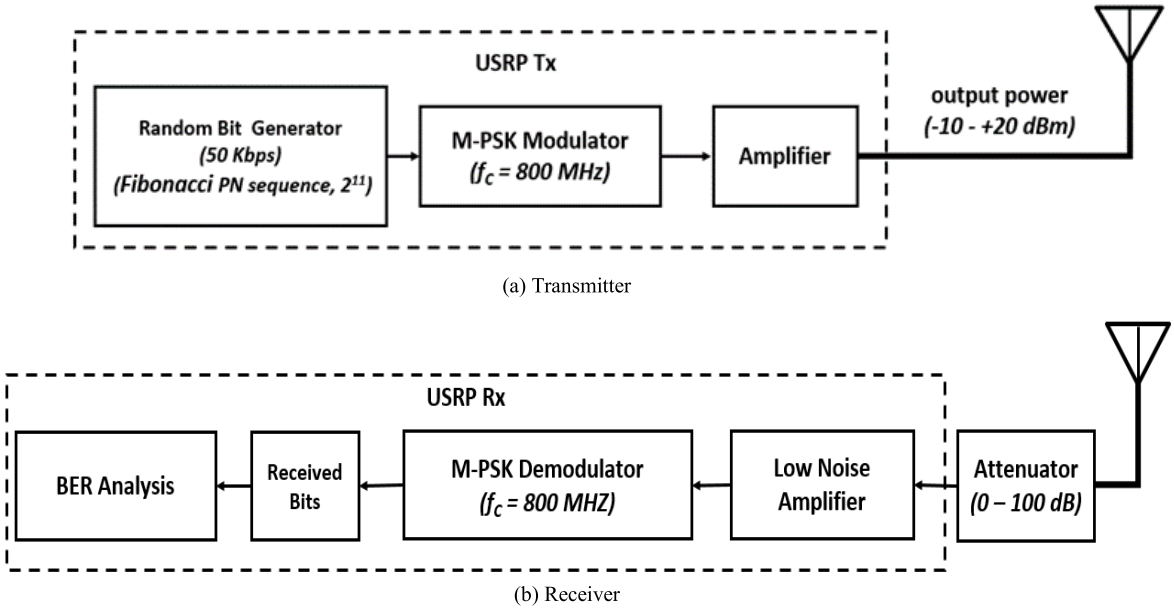

FIGURE 10. The standard MPSK USRP model.

is used, the transmitted signal cannot be recovered correctly due to distortion. Therefore, the modified MPSK modulator structure was designed for the harmonic modulated MPSK data transmission. Using the proposed method, the phase value of the standard MPSK modulation is modified in accordance with the modulation order. Thus, the variation in the constellation diagram is provided by the modified MPSK modulator. When applied in this way, the transmitted signal is recovered considering a certain loss by using the standard MPSK demodulator at the receiver. Although the same blocks are used in the modified MPSK modulator, the phase information at the output of the MT PSK System Parameters Creation block which is used to specify PSK modulation parameters in LabVIEW is divided into two because the harmonic modulation is used to generate the second harmonic of the MPSK data at the transmitter output. Afterwards, a phase shift of π is applied. The resulting modified MPSK constellation diagram for BPSK and QPSK is shown in Fig. 13. The non-square constellation diagram of the modified QPSK in Fig. 13(b) affects the discrimination when the frequency multiplier is applied, and this effect is observed as a power penalty.

In Fig. 12, the carrier frequency at the transmitter is set to be half of the carrier frequency at the receiver, since the frequency multiplication factor, N, is taken as two. When examining the two designs given in Fig. 10 and Fig. 12, respectively, the difference between them is the MPSK modulator structure used and the carrier frequency of the transmitter. The carrier frequency values of the standard MPSK modulator and the modified MPSK modulator differ due to the frequency multiplication. For the standard MPSK modulator, the carrier frequency value is $fc = 800$ MHz, whereas for the modified MPSK modulator, $fc = 400$ MHz.

On the transmitter side, although the carrier frequency values and modulator structures are different, the receiver side is exactly the same for both modulators. In other words, recovery of the transmitted signal without any change in the receiver structure is achieved with certain power and performance loss.

B. EXPERIMENTAL SETUP FOR MMWAVE TRANSMISSION

The hardware setup process includes designing the upconverter and downconverter structures to implement the proposed method in the mmWave band. After the real time modeled standard and modified MPSK modulators using USRP, upconverter and downconverter were designed. Whereas different upconverters are designed for the regular MPSK data transmission and harmonic MPSK data transmission, the downconverter structures used for the two MPSK transmissions are designed to be the same. The reason why the upconverter structures differ is because the modulator used for the regular MPSK data transmission and the modulator used for the harmonic MPSK data transmission are different.

1) THE REGULAR MPSK DATA TRANSMISSION SYSTEM SETUP IN THE MMWAVE BAND

Fig. 14 shows the schematic diagram of the regular MPSK data transmission system in the mmWave band. As shown in the Fig. 14, the implementation of our regular MPSK data transmission at 30 GHz hardware setup uses the following components: USRP devices, subharmonic mixers, 2 dB RF attenuator, variable attenuator, amplifier, power divider, Phased locked dielectric resonator oscillator (PDRO), horn antenna, and proper types of cables for connection. Fig. 15

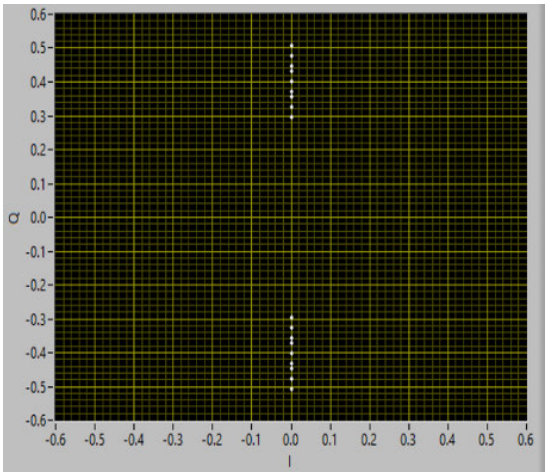

(a) BPSK

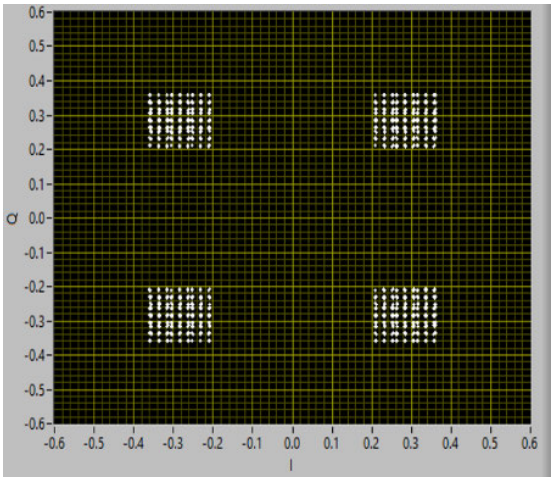

(b) QPSK

FIGURE 11. The constellation diagrams of the standard MPSK modulator in the LabVIEW environment.

shows the hardware setup of our regular MPSK data transmission system at 30 GHz.

On the transmitter side, the computer is connected to the NI USRP-2922 model USRP device via Ethernet cable. The USRP Tx device provides output by converting the digital signal to an analog intermediate frequency (IF) signal. Using the model designed for the standard MPSK modulator, the MPSK signal, which has a carrier frequency of 800 MHz at 50 kbps data rates at the output of the USRP Tx device, is transmitted as an input signal to the designed 30 GHz upconverter structure. Hertley CTI phase locked PDRO is used to generate the LO signal in the 30 GHz upconverter structure. A LO signal with 13 dBm RF output power is obtained at 15.2 GHz frequency at the PDRO output. The Picosecond 6 dB power divider is used so that the LO signal at the PDRO output can be used on the receiver side to provide coherent modulation. The PDRO output is connected to the first port of the power divider. Since the power divider used has 6 dB insertion loss, the LO signal is observed as 7 dBm at the outputs of the second and the third ports. The LO signal at the output of the power divider is connected to the input of the Mini Circuits coaxial wideband amplifier with a gain of 13 dB and an average output power of 18 dBm, operating in the frequencies between 5 GHz and 15 GHz. The purpose of using the amplifier here is to isolate the LO signal from the subharmonic mixer in order to prevent it from being reflected back. There is a 2 dB attenuator at the amplifier output. The attenuator is used to prevent the LO signal at the amplifier output from damaging the Miteq SBE0440LW1 Even Harmonic Balanced Mixer. Since the mixer operating in the frequencies between 4 GHz and 40 GHz has an LO power range from 10 dBm to 15 dBm, an attenuator is used in case of a signal with a power higher than 15 dBm at the amplifier output. As a result of the measurements made using the power detector, a signal which has power of 7 dBm is obtained at the attenuator output. The even harmonic balanced mixer achieves efficient RF to IF or IF to RF conversion using an LO at 1/2 the normal frequency. Thus, with the 15.2 GHz LO signal obtained, MPSK data at carrier frequency of 800 MHz coming from the USRP Tx device is converted into mmWave signal using an even harmonic balanced mixer with 9 dB conversion loss operating in the 4 GHz-40 GHz frequency range. The signal measured at the RF output has a power of 3 dBm at 30.4 GHz. Finally, the mixer output is connected to a horn antenna operating in the 26.5 GHz–40 GHz frequency range. The horn antenna has 20 dB gain. The collimator lenses are used to increase the strength of the signal transmitted.

On the receiver side, upconverted MPSK data transmitted in the mmWave band is sent to the downconverter using a horn antenna operating in the frequency range of 26.5 GHz-40 GHz, as shown in Fig. 14. The Rx power measurement was made by using a power detector at the antenna output. A variable attenuator, which can be adjusted in the range of 0 dB-69 dB, was used to perform performance analysis at different received power values. The variable attenuator output is connected to Miteq SBE0440LW1 Even Harmonic Balanced Mixer RF port to convert RF signal to IF signal. With the 15.2 GHz LO signal coming from the third port of the power divider used on the transmitter side, the RF signal at the variable attenuator output is downconverted. Then, the mixer IF signal is sent to the USRP Rx device, the IF signal is converted into a baseband signal by the USRP. The baseband signal processing and performance analysis of the system are performed to recover the signal and decode the original data packet. In addition, power budget analysis of the regular MPSK data transmission system has been performed to estimate the received power. During the analysis, various parameters were computed, including transmitted and received signal power, free space path loss (FSL), effective isotropic radiated power (EIRP), received isotropic power, thermal noise power, and received carrier to noise ratio (CNR). The losses of the components utilized in the mmWave communication system, such as conversion loss and insertion loss, were also considered. Table 1 contains the values of the parameters that were obtained as a result of the power budget analysis.

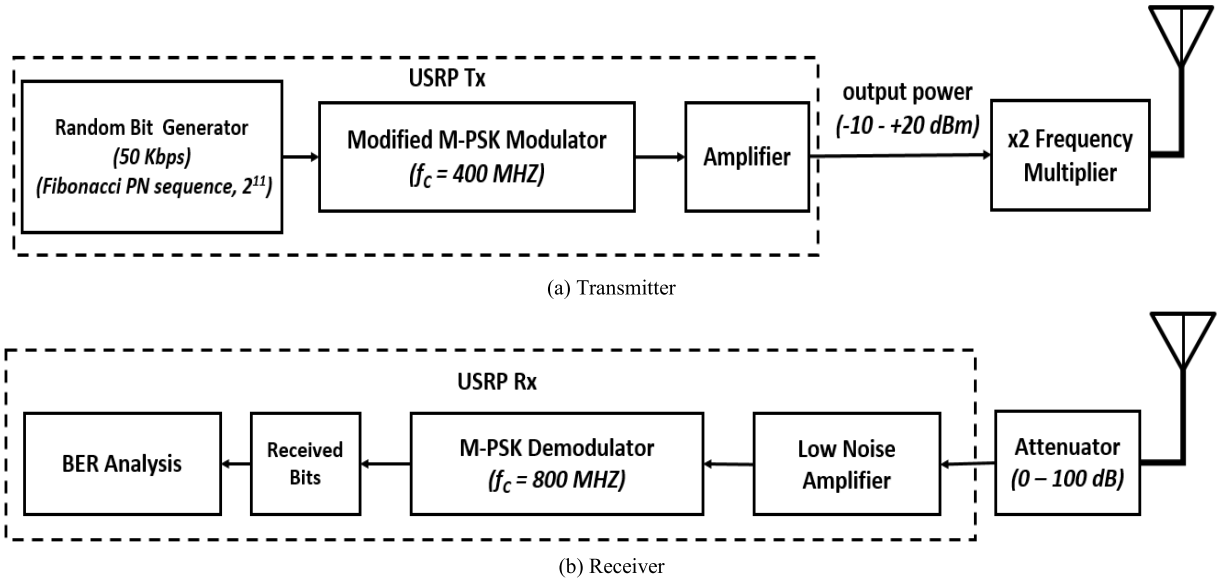

FIGURE 12. The modified MPSK USRP model.

TABLE 1. Power budget analysis of the regular MPSK data transmission system in MMwave band.

Symbol	Description	Value
P_t	Transmit Power (dBW)	-27 dBW
G_t	Transmitter antenna gain (dB)	20 dB
FSL	Free Space Path Loss (dB)	-57.66 dB
EIRP	Effective Isotropic Radiated Power (dBW)	-7 dBW
	Received Isotropic Power (dBW)	-64.66 dBW
G_r	Receiver antenna gain(dB)	10 dB
P_r	Received signal Power (dBW)	-54.66 dBW
N_0	Noise Spectral Density(dBW/Hz)	-203.8 dBW/Hz
k	Boltzman's constant (dBW/K-Hz)	-228.6 dBW/K-Hz
N	Thermal Noise Power (dBW)	-156,838 dBW
	Received Pr/No (dB-Hz)	102.178 dB-Hz
	Data Rate (dB-bit/s)	46.99 dB-bit/s
CNR	Received CNR (dB)	55.18 dB

2) THE HARMONIC MPSK DATA TRANSMISSION SYSTEM SETUP IN THE MMWAVE BAND

Fig. 16 shows the schematic diagram of the harmonic MPSK data transmission system in the mmWave band. As shown in the Fig. 16, the implementation of our harmonic MPSK data transmission at 30 GHz hardware setup uses the following components: USRP devices, mixer, subharmonic mixer, variable attenuator, power divider, PDRO, frequency multiplier, horn antenna, and proper types of cables for connection. Fig. 17 shows the hardware setup of our harmonic MPSK data transmission system at 30 GHz.

On the transmitter side, the computer is connected to the NI USRP-2922 model USRP device via Ethernet cable. Using the model designed for the modified MPSK modulator, the MPSK signal, which has a carrier frequency of 400 MHz at 50 kbps data rates at the output of the USRP Tx device, is transmitted as an input signal to the designed 30 GHz upconverter structure. Hertley CTI phase locked PDRO is used to generate the LO signal in the 30 GHz upconverter structure. A LO signal with 13 dBm RF output power is obtained at 15.2 GHz frequency at the PDRO output. The Picosecond 6 dB power divider is used so that the LO signal at the PDRO output can be used on the receiver side to provide coherent modulation. Since the power divider used has 6 dB insertion loss, the LO signal power is observed as 7 dBm at the outputs of the second and third ports. The LO signal at the output of the power divider is connected to the input of the mixer.

Miteq DM0520LW1 Double Balanced mixer is used in the transmitter. This mixer works in the frequency range of 5 GHz-20 GHz and has a conversion loss of 5 dB. The modified MPSK data sent from the USRP Tx device is upconverted with the 15.2 GHz LO signal at the power divider output. After the measurement, a signal at a frequency of 15.2 GHz with 2 dBm power was observed at the mixer output. Unlike the studies in the literature, frequency multiplication method was used at this stage for the harmonic modulation of the signal at the mixer output. With harmonic modulation, the transmission of modified MPSK data was implemented. For the harmonic modulation, Analog Devices HMC577LC4B Active frequency multiplier operating in the 13.5 GHz-15.5 GHz input frequency range and 27 GHz-31 GHz output frequency range is used. Also, an output power of 20 dBm can be obtained at the frequency multiplier output. However, as a result of the measurement, a signal with 8 dBm power was obtained at the frequency multiplier output. The modified MPSK data at 400 MHz carrier frequency coming from the USRP Tx device is converted into mmWave signal using the frequency multiplication. Finally, the frequency multiplier output is connected to a horn antenna operating

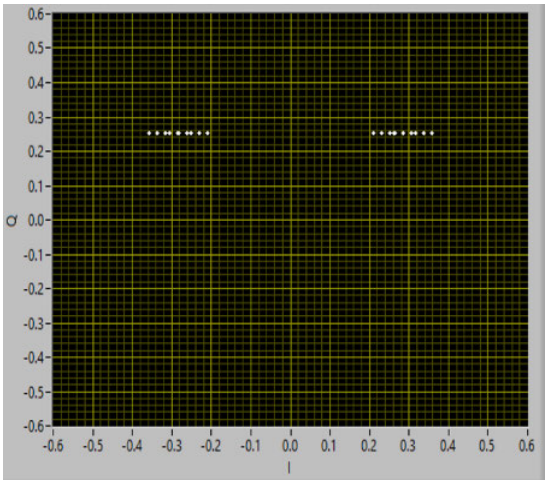

(a) Modified BPSK

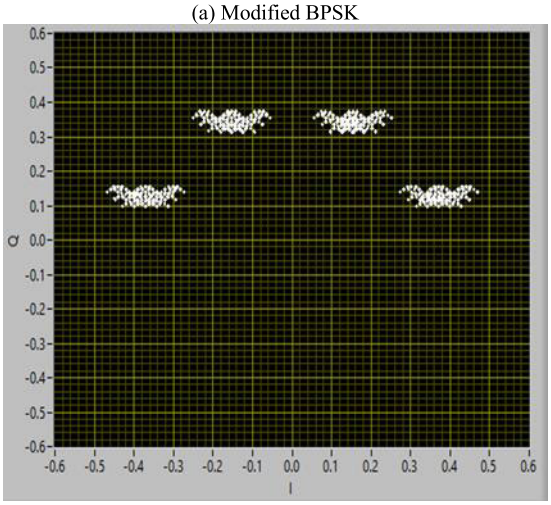

(b) Modified QPSK

FIGURE 13. The constellation diagrams of the modified MPSK modulator in the LabVIEW environment.

in the 26.5 GHz–40 GHz frequency range. The transmitting horn antenna has 20 dB gain. The collimator lenses are used to increase the strength of the signal transmitted between the transmitter and the receiver.

On the receiver side, upconverted MPSK data transmitted in the mmWave band is sent to the downconverter using a horn antenna operating in the frequency range of 26.5 GHz-40 GHz, as shown in Fig. 16. The receiving horn antenna has 10 dB gain. The Rx power measurement was made by using a power detector at the antenna output. The variable attenuator adjustable in the range of 0 dB-69 dB was used to perform error performance analysis at different received power values. The variable attenuator output is connected to Miteq SBE0440LW1 Even Harmonic Balanced Mixer RF port to convert RF signal to IF signal. With the 15.2 GHz LO signal coming from the third port of the power divider used on the transmitter side, the RF signal at the variable attenuator output is downconverted. Then, the mixer IF signal is sent to the USRP Rx device, the IF signal is converted into a baseband signal by the USRP. The baseband signal processing and error performance analysis of the system

TABLE 2. Power budget analysis of the harmonic MPSK data Transmission System in MMwave band.

Symbol	Description	Value
P_t	Transmit Power (dBW)	-22 dBW
G_t	Transmitter antenna gain (dB)	20 dB
FSL	Free Space Path Loss (dB)	-57.66 dB
EIRP	Effective Isotropic Radiated Power (dBW)	-2 dBW
	Received Isotropic Power (dBW)	-59.66 dBW
G_r	Receiver antenna gain(dB)	10 dB
P_r	Received signal Power (dBW)	-49.66 dBW
N_0	Noise Spectral Density(dBW/Hz)	-203.8 dBW/Hz
k	Boltzman's constant (dBW/K-Hz)	-228.6 dBW/K-Hz
N	Thermal Noise Power (dBW)	-156,838 dBW
	Received Pr/No (dB-Hz)	107.178 dB-Hz
	Data Rate (dB-bit/s)	46.99 dB-bit/s
CNR	Received CNR (dB)	60.18 dB

are performed to recover the signal and decode the original data packet. Furthermore, similar to the regular MPSK data transmission system, an analysis of the power budget has been conducted for the harmonic MPSK data transmission system to estimate the received power.

Table 2 contains the values of the parameters that were obtained as a result of the power budget analysis.

IV. RESULTS

The LOS measurements for the performance of the proposed system in this study were carried out in the indoor laboratory environment for 30 GHz mmWave data transmission in two different scenarios. These are regular MPSK data transmission and harmonic MPSK data transmission scenarios. The LOS measurements of these two scenarios in the indoor environment were accomplished, that include setup of the mmWave data transmission systems and, as well as the description of the proposed scheme. The LOS measurements made for a distance of 60 centimeters between the transmitting and receiving antenna were analyzed in terms of the received power. The received power measurements were made by attaching a RF power detector to the receiver antenna output for both the regular MPSK and the harmonic MPSK data transmission. The received power and the results of the BER performance of the mmWave transmission systems were compared. The BER measurements were made using the MT BER Calculate block in the modulation toolkit of the LabVIEW program. The BER measurement results for the regular MPSK data transmission and the harmonic MPSK data transmission modulations for $M = 2$, and $M = 4$ are shown in Fig. 18.

In Fig. 18, when the regular BPSK data transmission at 30 GHz is compared with the harmonic BPSK data transmission at 30 GHz, a power penalty of 2.3 dB is observed. Likewise, it was concluded that the 30 GHz harmonic QPSK data transmission combined with the proposed method showed a noteworthy error performance improvement. The reasons behind the power penalty are phase noise in the

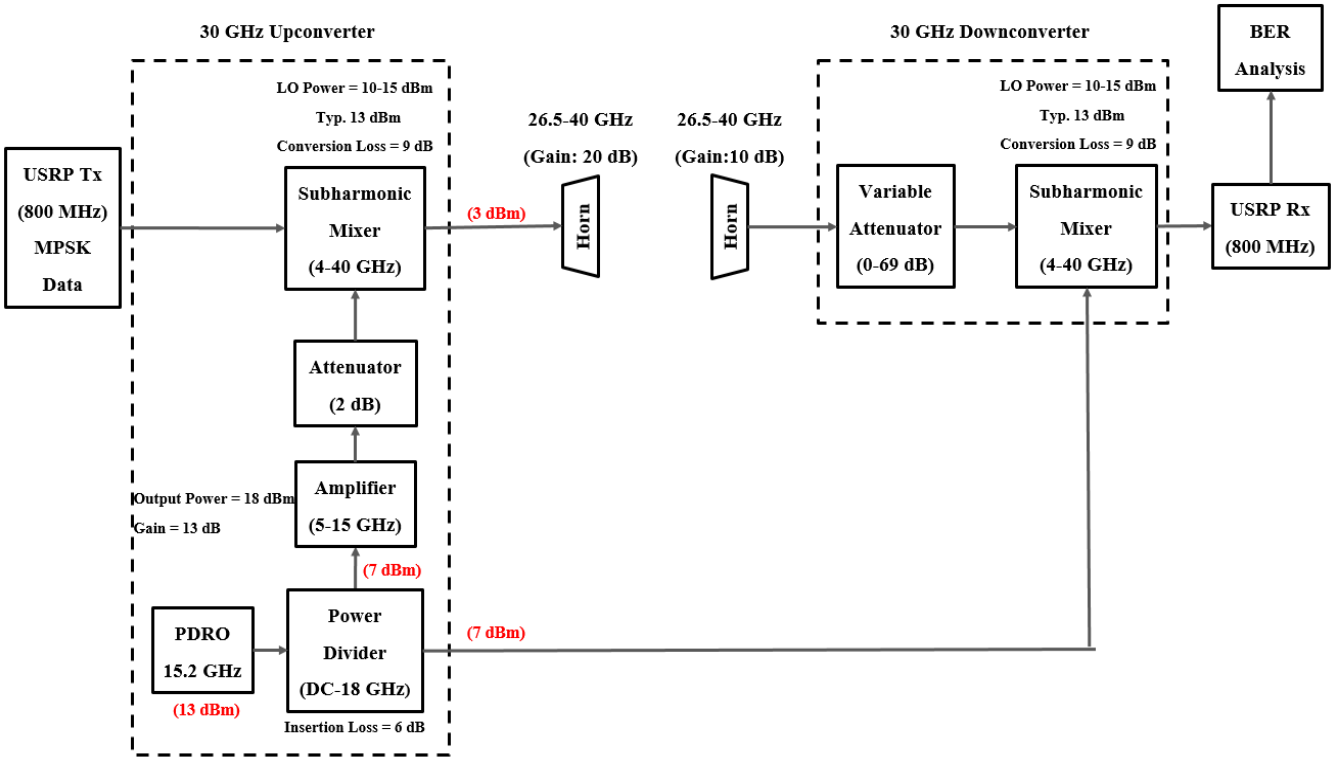

FIGURE 14. Schematic diagram of our mmWave experimental setup for regular MPSK.

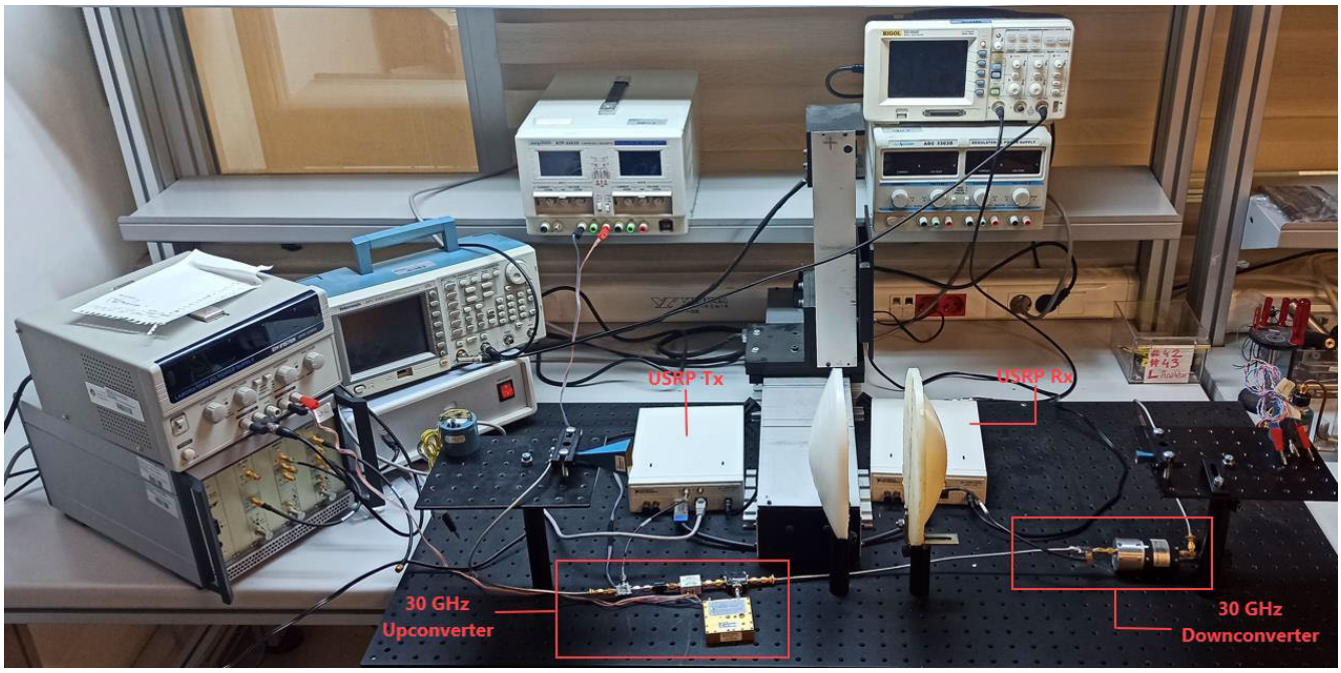

FIGURE 15. Experimental setup for regular MPSK transmission system at 30 GHz.

oscillator and the PLL in the receiver. Both experimental systems are affected by the phase noise resulting from the oscillator. In the harmonic MPSK data transmission system, constellation modification and frequency multiplication methods are used. When the MPSK signal is multiplied by a factor of N, the phase noise increases N times, which affects the BER performance of the system. Moreover, the frequency multiplication causes a change in the phase response of the filter when a standard bandpass filter is used during modulation. This leads to filter mismatch even if a standard

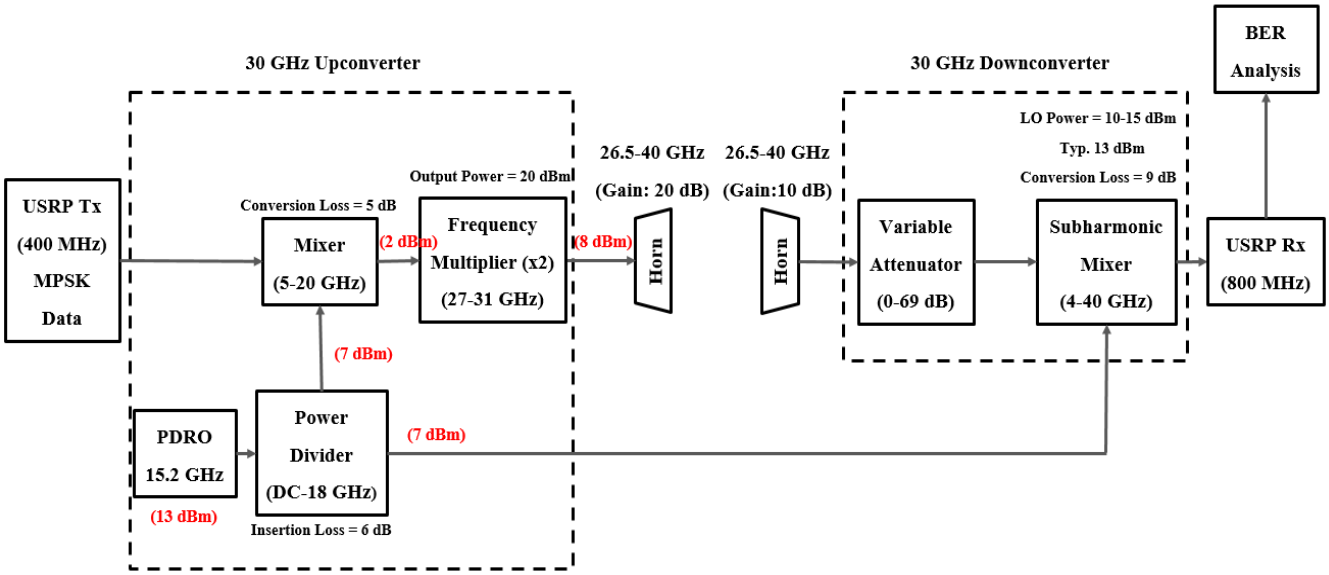

FIGURE 16. Schematic diagram of our mmWave experimental setup for harmonic MPSK.

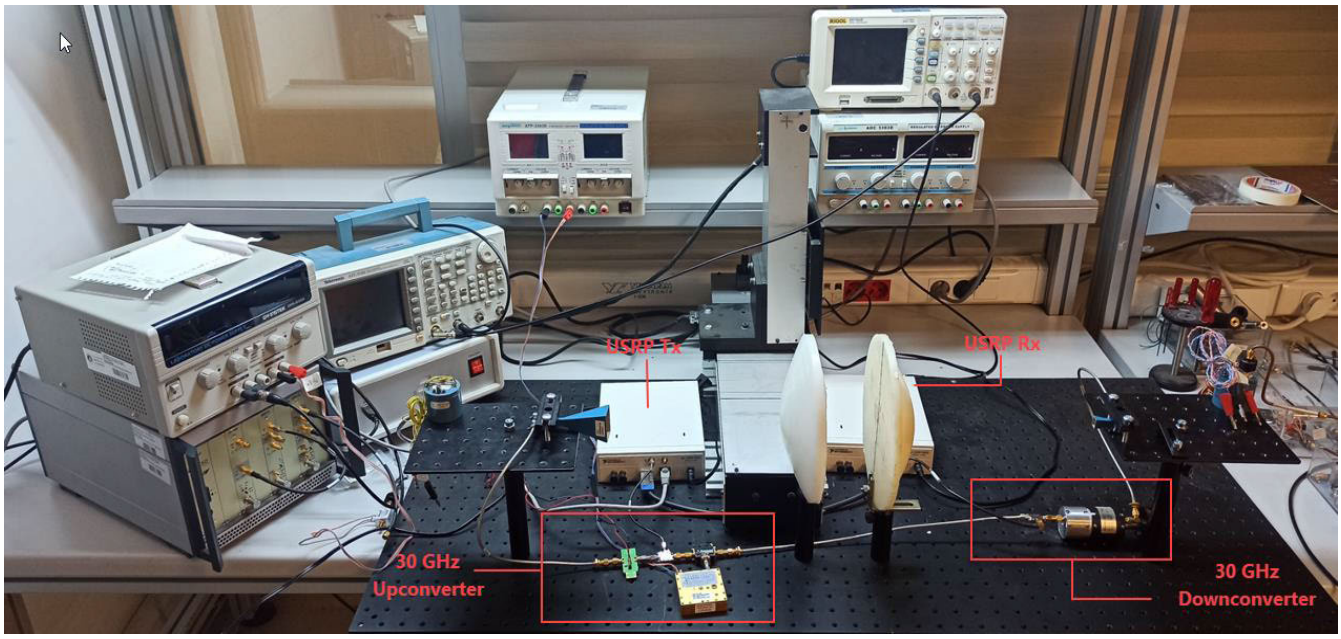

FIGURE 17. Experimental setup for harmonic MPSK transmission system at 30 GHz.

bandpass filter is utilized in the receiver. The theoretical BER analysis in Section II-C shows the effect of phase noise on the harmonic MPSK signal. Additionally, simulations were conducted in MATLAB for regular and harmonic BPSK transmission with and without phase noise over an AWGN channel, and the results in Fig. 9 were obtained. In summary, both experimental and simulation results confirm that phase noise causes a reduction in BER performance of the harmonic MPSK system and a non-negligible power penalty. However, there are several techniques available to mitigate the effect of phase noise. The use of high quality oscillators is crucial in reducing the level of phase noise. Additionally, a PLL can be designed to maintain a constant phase relationship between the signal and the oscillator, thereby reducing the effect of phase noise. Narrowband filters can improve the SNR by rejecting frequencies outside a specific range. Utilizing suitable modulation schemes, as well as channel encoding, can be provided to be robust to phase noise. Finally, equalization techniques and different estimator types such as LS, ML and Kalman filter can also be used to mitigate phase noise in communication systems. Overall, the approach to mitigate phase noise should be determined depend on

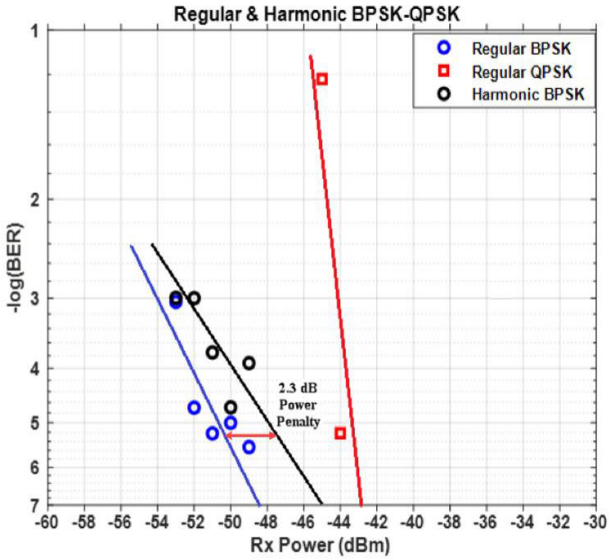

FIGURE 18. BER comparison for measurements of the regular and the harmonic MPSK data transmission at 30 GHz.

the requirements of the communication system. Therefore, a combination of the above techniques may be necessary to achieve optimal performance.

V. CONCLUSION

In this study, we have proposed a novel constellation modification method for MPSK data transmission with frequency multiplication technique, which offers an important solution in providing transmission in mmWave band to meet high data rates and capacity demand. In order to provide transmission in the mmWave band, unlike the modulation process performed after the frequency of the LO signal is moved to the mmWave band using a frequency multiplier, the modulated signal is transferred to the high frequency band using the frequency multiplication method. In addition, MPSK modulation is used instead of the square wave On-Off modulation typically used in the transmitter, which is slightly affected by frequency multiplication. The nonlinear effect caused by the frequency multiplication makes it difficult to recover the data in the receiver for the phase modulation types, and the proposed constellation modification method is applied in the transmitter to solve the data recovery problem. In this way, MPSK transmission was carried out with a modified constellation for the harmonic modulation, which was created without the need for higher bandwidth or digital processing load and without changing the receiver structure.

For the mmWave testbed of the regular and the harmonic MPSK data transmission, the transmitter and receiver blocks were developed in the LabVIEW environment and tested using NI USRP-2922 models. The BER results for measurements of the regular and harmonic MPSK data transmissions have been obtained.

The frequency multiplication method applied in the transmitter for data transmission at high data rates in the mmWave band and the novel constellation modification method proposed for the implementation of harmonic modulation on MPSK data, will make a significant contribution to adopt the system to modulation types with high modulation order. In addition, it has been shown that the proposed method can be applied on modulated data for experimental studies to be carried out in the mmWave band using the frequency multiplier chain.

REFERENCES

[1] S. Ju, Y. Xing, O. Kanhere, and T. S. Rappaport, "Millimeter wave and sub-terahertz spatial statistical channel model for an indoor office building," *IEEE J. Sel. Areas Commun.*, vol. 39, no. 6, pp. 1561–1575, Jun. 2021.

[2] M. Xiao, S. Mumtaz, Y. Huang, L. Dai, Y. Li, M. Matthaiou, G. K. Karagiannidis, E. Björnson, K. Yang, and A. Ghosh, "Millimeter wave communications for future mobile networks," *IEEE J. Sel. Areas Commun.*, vol. 35, no. 9, pp. 1909–1935, Sep. 2017.

[3] H. Zhang, Y. Zhang, J. Cosmas, N. Jawad, W. Li, R. Muller, and T. Jiang, "MmWave indoor channel measurement campaign for 5G new radio indoor broadcasting," *IEEE Trans. Broadcast.*, vol. 68, no. 2, pp. 331–344, Jun. 2022.

[4] X. Wang, L. Kong, F. Kong, F. Qiu, M. Xia, S. Arnon, and G. Chen, "Millimeter wave communication: A comprehensive survey," *IEEE Commun. Surveys Tuts.*, vol. 20, no. 3, pp. 1616–1653, 3rd Quart., 2018.

[5] Y. J. Kim, Q. Sultan, and Y. S. Cho, "Pilot sequence design for mmWave cellular systems with relay stations in the presence of blockage," *IEEE Access*, vol. 8, pp. 80454–80467, 2020.

[6] T. Liu, J. Lu, J. Ma, Y. Wang, and J. Liu, "Spectral shaped PAM4 signal based on nonlinear differential coding for AOWC system with self-pumping structure," *Opt. Fiber Technol.*, vol. 73, Oct. 2022, Art. no. 103061.

[7] Z. Chen, C. Han, Y. Wu, L. Li, C. Huang, Z. Zhang, G. Wang, and W. Tong, "Terahertz wireless communications for 2030 and beyond: A cutting-edge frontier," *IEEE Commun. Mag.*, vol. 59, no. 11, pp. 66–72, Nov. 2021.

[8] Ö. Ersoy and A. B. Sahin, "Investigation of harmonic frequency multiplication on transmitted data through pulse shaping for 6G communication," in *Proc. 7th Int. Conf. Electr. Electron. Eng. (ICEEE)*, Antalya, Turkey, Apr. 2020, pp. 237–242.

[9] ö. Ersoy, M. C. Karakoç, and v. A. B. sahin, "Investigation of faster than Nyquist transmission for terahertz communication using harmonic receiver," in *Proc. 29th Signal Process. Commun. Appl. Conf. (SIU)*, Istanbul, Turkey, Jun. 2021, pp. 1–4.

[10] K. Du, O. Ozdemir, F. Erden, and I. Guvenc, "Sub-terahertz and mmWave penetration loss measurements for indoor environments," in *Proc. IEEE Int. Conf. Commun. Workshops (ICC Workshops)*, Montreal, QC, Canada, Jun. 2021, pp. 1–6.

[11] R. Muller, S. Hafner, D. Dupleich, J. Luo, E. Schulz, R. Herrmann, C. Schneider, R. S. Thoma, X. Lu, and T. Wang, "Ultra-wideband channel sounder for measurements at 70 GHz," in *Proc. IEEE 81st Veh. Technol. Conf. (VTC Spring)*, Glasgow, U.K., May 2015, pp. 1–5.

[12] Y. Li, Y. Wang, Y. Chen, Z. Yu, and C. Han, "Channel measurement and analysis in an indoor corridor scenario at 300 GHz," in *Proc. IEEE Int. Conf. Commun.*, May 2022, pp. 2888–2893.

[13] T. Kurner, D. M. Mittleman, and T. Nagatsuma, *THz Communications: Paving the Way Towards Wireless Tbps*, vol. 234. Cham, Switzerland: Springer, 2022.

[14] P. F. Goldsmith, "How 50 years of technology development has transformed millimeter-THz astronomical spectroscopy," in *Proc. 46th Int. Conf. Infr., Millim. Terahertz Waves (IRMMW-THz)*, Chengdu, China, Aug. 2021, pp. 1–7.

[15] H. J. Song and T. Nagatsuma, *Handbook of Terahertz Technologies: Devices and Applications*, 1st ed. Boca Raton, FL, USA: CRC Press, 2015.

[16] H. Yang, H. Mou, C. Sun, Z. Guo, X. Liu, S. Ding, X. Zou, and X. Gao, "E-band propagation measurements and initial analysis for long-range communication over sea," in *Proc. 3rd Int. Conf. Geol., Mapping Remote Sens. (ICGMRS)*, Zhoushan, China, Apr. 2022, pp. 828–832.

[17] B. Schoch, F. Wiewel, D. Wrana, L. Manoliu, S. Haussmann, A. Tessmann, and I. Kallfass, "Performance optimization of an E-band communication link using open-loop predistortion," in *Proc. 14th German Microw. Conf. (GeMiC)*, Ulm, Germany, May 2022, pp. 216–219.

[18] (2022). *60 GHz Wavequide Transmitter/Receiver Modules and Development System New From Pasternack*. [Online]. Available: https://www.pasternack.com/n-pasternack-introduces-60-ghz-waveguide-modules-and-development-system.aspx
[19] (2022). *60 GHz RF Transceiver A2 Family*. [Online]. Available: https://www.st.com/en/wireless-connectivity/st60a2g0.html
[20] (2022). *Transceiver Chips Corral mmWaves*. [Online]. Available: https://www.analog.com/en/technical-articles/transceiver-chips.html
[21] (2022). *Fujikura Millimeter-Wave Wireless Communications Module*. [Online]. Available: https://mmwavetech.fujikura.jp/
[22] S. M. Hashir, "PSK modulation/demodulation and performance evaluation in FM BAND USINg USRP," in *Proc. Adv. Wireless Opt. Commun. (RTUWO)*, Riga, Latvia, 2018, pp. 66–71.
[23] (2022). *5G Massive MIMO Testbed: From Theory to Reality*. [Online]. Available: https://www.ni.com/en-tr/innovations/white-papers/14/5g-massive-mimo-testbed–from-theory-to-reality–.html
[24] L. Y. Hosni, A. Y. Farid, A. A. Elsaadany, and M. A. Safwat, "5G new radio prototype implementation based on SDR," *Commun. Netw.*, vol. 12, no. 1, pp. 1–27, Feb. 2020.
[25] M. Danneberg, R. Bomfin, A. Nimr, Z. Li, and G. Fettweis, "USRP-based platform for 26/28 GHz mmWave experimentation," in *Proc. IEEE Wireless Commun. Netw. Conf. Workshops (WCNCW)*, Seoul, (South) Korea, Apr. 2020, pp. 1–6.
[26] A. Quadri, H. Zeng, and Y. T. Hou, "A real-time mmWave communication testbed with phase noise cancellation," in *Proc. IEEE INFOCOM Conf. Comput. Commun. Workshops (INFOCOM WKSHPS)*, Paris, France, Apr. 2019, pp. 455–460.
[27] G. H. Sim, A. Asadi, A. Loch, M. Hollick, and J. Widmer, "Opp-relay: Managing directionality and mobility issues of millimeter-wave via D2D communication," in *Proc. 9th Int. Conf. Commun. Syst. Netw. (COMSNETS)*, Bengaluru, India, Jan. 2017, pp. 144–151.
[28] M. Hofer, D. Löschenbrand, J. Blumenstein, H. Groll, S. Zelenbaba, B. Rainer, L. Bernadó, J. Vychodil, T. Mikulasek, E. Zöchmann, S. Sangodoyin, H. Hammoud, B. Schrenk, R. Langwieser, S. Pratschner, A. Prokes, A. F. Molisch, C. F. Mecklenbräuker, and T. Zemen, "Wireless vehicular multiband measurements in centimeterwave and millimeterwave bands," in *Proc. IEEE 32nd Annu. Int. Symp. Pers., Indoor Mobile Radio Commun. (PIMRC)*, Helsinki, Finland, Sep. 2021, pp. 836–841.
[29] C. Jin, "GaN Schottky diodes for signal generation and control," Ph.D. dissertation, Dept. Elect. Eng. Inf. Technol., Tech. Univ. Darmstadt, Darmstadt, Germany, 2015.
[30] M. Viswanathan, *Simulation of Digital Communication Systems Using MATLAB*. Smashwords, 2013.
[31] T. S. Rappaport, *Wireless Communications Principles and Practice*, 1st ed. Upper Saddle River, NJ, USA: Prentice-Hall, 2002.
[32] Y. Jang, J. Jeong, and D. Yoon, "Bit error floor of MPSK in the presence of phase error," *IEEE Trans. Veh. Technol.*, vol. 65, no. 5, pp. 3782–3786, May 2016.
[33] C. Bicici, I. Ozdur, and O. Cerezci, "Analysis of oscillator phase noise effect on high order QAM links," *Anal. Integr. Circuits Signal Process.*, vol. 105, no. 1, pp. 1–6, Oct. 2020.
[34] T. V. Pham, T. V. Nguyen, and A. T. Pham, "A general conditional BER expression of rectangular QAM in the presence of phase noise," in *Proc. IEEE 32nd Annu. Int. Symp. Pers., Indoor Mobile Radio Commun. (PIMRC)*, Sep. 2021, pp. 422–427.
[35] S. Ahn, S. An, H. Oh, and D. Yoon, "Approximate closed-form expression for the average BER of M-ary PSK with Gaussian-distributed phase error," in *Proc. 27th Int. Conf. Telecommun. (ICT)*, Bali, Indonesia, Oct. 2020, pp. 1–4.
[36] X. Deng, H. Yang, Q. Wu, J. Jiang, and C. Lin, "Phase noise effects on the performance of high-order digital modulation terahertz communication system," *Chin. J. Electron.*, vol. 31, no. 3, pp. 589–594, May 2022.
[37] D. Taggart and R. Kumar, "Impact of phase noise on the performance of the QPSK modulated signal," in *Proc. Aerosp. Conf.*, Big Sky, MT, USA, Mar. 2011, pp. 1–10.
[38] Y. Jang, D. Yoon, and S.-K. Lee, "Generalized BER expression of MPSK in the presence of phase error," *IEEE Commun. Lett.*, vol. 17, no. 12, pp. 2213–2216, Dec. 2013.
[39] H. Jafari, H. Miar-Naimi, and J. Kazemitabar, "Bit error probability of MQAM in the presence of phase noise," *IEEE Trans. Veh. Technol.*, vol. 69, no. 12, pp. 14918–14931, Dec. 2020.
[40] P. Desombre, H. Farès, and Y. Louet, "Performance comparison of digital modulations in the presence of Gaussian phase noise in the sub-THz context," in *Proc. 4th Int. Workshop Mobile Terahertz Syst. (IWMTS)*, Essen, Germany, Jul. 2021, pp. 1–5.
[41] Y. Jang, "Average BER performance of MPSK with noisy phase reference in Nakagami-*m* fading channel," *Electron. Lett.*, vol. 57, no. 21, pp. 823–825, Oct. 2021.
[42] P. E. G. Silva, R. A. A. de Souza, D. B. da Costa, J. M. Moualeu, and M. D. Yacoub, "Error probability of M-phase signaling with phase noise over fading channels," *IEEE Trans. Veh. Technol.*, vol. 69, no. 6, pp. 6766–6770, Jun. 2020.
[43] F. Munier, E. Alpman, T. Eriksson, A. Svensson, and H. Zirath, "Estimation of phase noise for QPSK modulati on over AWGN channels," in *Proc. GigaHertz, 7th Symp., Linköping Electron. Conf.*, 2003.
[44] A. Chandra, A. Patra, and C. Bose, "Performance analysis of BPSK over different fading channels with imperfect carrier phase recovery," in *Proc. IEEE Symp. Ind. Electron. Appl. (ISIEA)*, Penang, Malaysia, Oct. 2010, pp. 106–111.
[45] A. Chandra, D. Biswas, and C. Bose, "BER performance of coherent PSK in Rayleigh fading channel with imperfect phase estimation," in *Proc. Int. Conf. Recent Trends Inf., Telecommun. Comput.*, Kerala, India, Mar. 2010, pp. 130–134.

ÖZGÜN ERSOY was born in Aydin, Turkey, in 1989. He received the B.S. degree in electronics and communication engineering from Kocaeli University, Kocaeli, Turkey, in 2012, and the M.S. degree in electrical and electronics engineering from Ankara Yıldırım Beyazıt University, Ankara, Turkey, in 2017, where he is currently pursuing the Ph.D. degree with the Department of Electrical and Electronics Engineering. His current research interests include wireless communication, millimeter wave and terahertz frequency communication, modulation methods, and channel access methods.

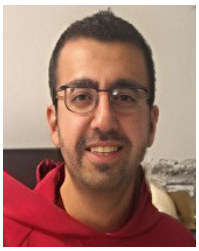

MURAT CAN KARAKOÇ received the B.S. degree in electrical and electronics engineering from Eskişehir Osmangazi University, Eskişehir, Turkey, in 2015, and the M.S. degree from Ankara Yıldırım Beyazıt University, Ankara, Turkey, in 2018, where he is currently pursuing the Ph.D. degree. His current research interests include wireless communication, millimeter wave and terahertz frequency communication, modulation methods, and quantum sensing.

ASAF BEHZAT ŞAHİN received the B.S. degree in electrical and electronics engineering from Middle East Technical University, Ankara, Turkey, in 1996, and the M.S. and Ph.D. degrees from the University of Southern California, Los Angeles, CA, USA, in 1998 and 2003, respectively.

He was a part time consultant on optical systems for several Silicon Valley companies, until 2004. He joined the Faculty of Electrical and Electronics Engineering, Middle East Technical University, in 2004, where he was an Assistant Professor, until 2012. He also gave lectures in Air War College, Istanbul, and Middle East Technical University, Northern Cyprus Campus. Since 2012, he has been with the Electrical and Electronics Engineering Department, School of Engineering and Natural Sciences, Ankara Yıldırım Beyazıt University, Ankara. He has participated in more than 40 research and development projects. He is currently a researcher and a principal investigator of projects in the fields of terahertz spectrometry, non-destructive acoustic, and optical testing for quality, millimeter and sub-millimeter wave remote imaging for security, millimeter wave and terahertz frequency communication systems, fiber optical distributed acoustic sensors, and MEMS integrated fiber microphone. He has two international patents in the field of optical communications, and more than 100 research publications and conference proceedings in various fields. His major research interests include fiber optics, communication, quantum cryptography, terahertz, millimeter waves, and remote imaging.